Journal of Applied Electrochemistry **34**: 19–30, 2004.

Electromagnetic control of electroplating of a cylinder in forced convection

PEDRO OLIVAS[1,*], ANTOINE ALEMANY[1] and FRITZ H. BARK[2]
[1]*LEGI, BP53, 38041 Grenoble Cedex 9, France*
[2]*FaxénLaboratoriet, Kungl. Tekniska Högskolan, SE-100 44 Stockholm, Sweden*
*(*author for correspondence, e-mail: pedro.olivas@grenet.fr)*

Received 10 January 2003; accepted in revised from 31 July 2003

Key words: cylinder, electrochemical coating, electrodeposition, forced convection, magnetic field, magnetoelectrolysis, mass transport, numerical solutions

Abstract

Continuous electrodeposition on a cylindrical cathode, e.g. electrodeposition of gold on electrical connectors, is usually characterized by an undesirable non-homogeneity of the deposit thickness. This has been observed in industrial applications. Numerical simulations have shown very good agreement with observations. This paper deals with the possibility of improving the homogeneity of the deposit thickness by a magnetic field that is parallel to the axis of the cylinder. The electromagnetic volume force generated by such a magnetic field may set up a swirling motion around the cylinder. By controlling the force density it is possible to control the thickness of the diffusive layer and consequently the mass transfer. The magnetic field can be optimized with respect to strength, spatial extent and variation with time. It is shown that a strong alternating magnetic field of low frequency gives a nearly homogeneous deposit.

1. Introduction

In many electrochemical processes, mass transfer is the rate-controlling mechanism for a high voltage between the electrodes. This is the case in e.g. continuous electroplating processes for mass production of various products. A well known example is the 'reel-to-reel' electroplating of gold on electrical connectors. In electroplating, the near-wall hydrodynamics is crucial as it controls the diffusive boundary layer transport of the electroactive species to the body to be coated. The use of forced convection in continuous plating is often economically beneficial, as high deposition rates are obtained. Several large scale industrial applications are based on this concept. Examples are the continuous plating of zinc, chromium, and tin on steel strips, and the continuous deposition of copper foils used in e.g. the production of printed circuit boards.

When plating individual workpieces, like cylindrical connectors, forced convection usually distorts the distribution of the deposit and produces a significant difference between the thickness of the deposit layer at the upstream and downstream parts of a cylinder [1, 2]. To partially compensate for this disadvantage, turbulent lateral jets may improve the result [2]. Such jets improve the mass transfer rate but do not satisfactorily cure the non-uniform distribution of the deposit. An imposed swirling motion around the cylinder should result in a more homogeneous distribution of the mass transfer. However, it is hard to envisage a circulation around each cylinder in an array being set up by some mechanical device. This paper presents a different strategy for enforcing a local circulatory flow with the help of a magnetic field.

The effect of magnetic field application in electrochemistry is well known now as essentially based on the acceleration of overall mass transfer process induced by the solution flow. This flow is generated by the Lorentz force, which arises from the interaction between electrolytic current and magnetic field. The effects of an imposed magnetic field on electrolysis can somewhat crudely be subdivided into four classes: electrode-process kinetics, thermodynamic properties, surface morphology and mass transfer. Research on electrolytic mass transfer in a magnetic field has mainly focused on flat plates or rotating discs under static magnetic fields. For electrochemical mass transfer to a circular cylinder, comparatively few investigations are reported. Most of these focus on measurements of overall mass transfer coefficients, see e.g. [3–5].

In the present work, the effects of a magnetic field on mass transport and its coupling with a simple reaction mechanism at a cylindrical electrode are examined. These effects are caused by the modification of the motion of the electrolyte by the Lorentz force which arises from the interaction between the magnetic field and the electric current. A modified flow field will change the structure of the diffusion layer and hence the supply of reactants to the surface of the cylinder. The purpose of this study is to investigate the possibilities to even out, by imposing a magnetic field, the strong non-uniformity of the deposit that is shown in Figure 1. The

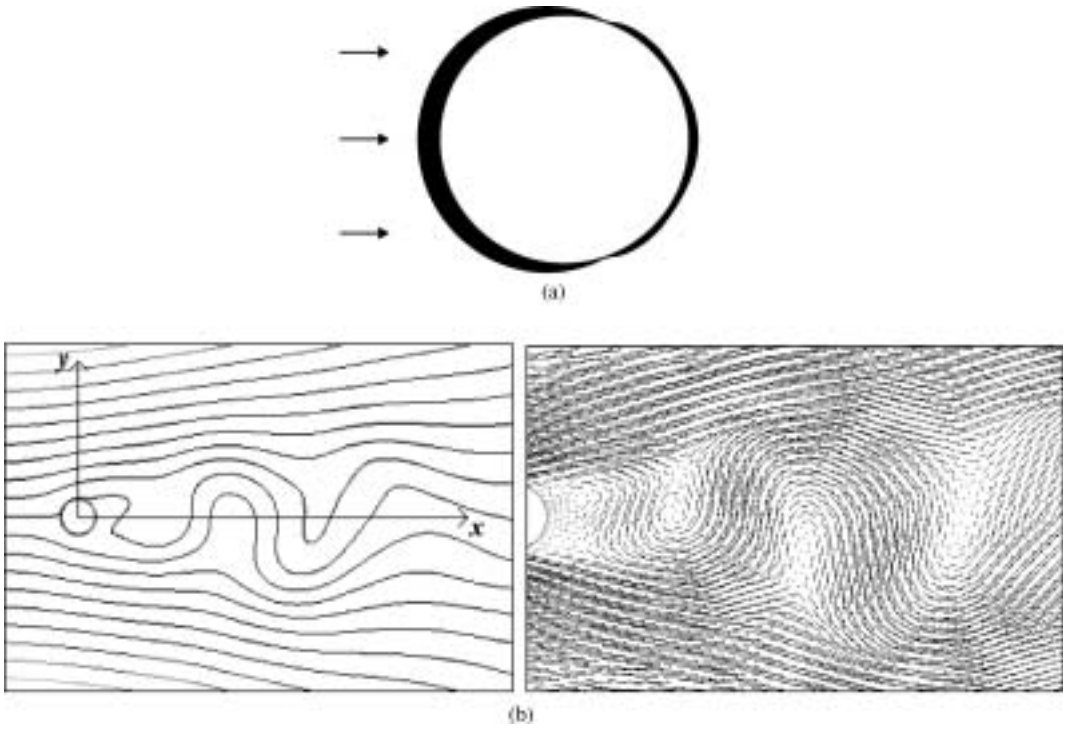

Fig. 1. (a) Enlarged deposit layer thickness on a cylinder from electroplating in forced convection without a magnetic field. The motion of the electrolyte is perpendicular to the axis of the cylinder. Limiting current state at $Re = 200$ [1]. (b) Instantaneous flow around a cylinder without magnetic field at $Re = 200$. Left: streamlines and coordinate system. Right: zoom on velocity vectors downstream of the cylinder.

magnetic field is taken to be parallel to the axis of the cylinder. The external control parameters are the intensity, the spatial distribution and temporal variation of the magnetic field.

2. Problem statement

The case studied in this work is a model of gold plating of male electric contact. In the industrial process, an array of cylinders is moving through a series of baths [5, 6]. In this study, however, as a first step, the plating process of a single cylinder is considered. The electrolyte is assumed to be dilute and contains one electroactive species and an excess of supporting electrolyte. Usually the major constituents of gold-plating baths are potassium cyanoaurate $K[Au(CN)_2]$ for supplying gold metal and the conducting salt is generally a phosphate or citrate-based formulation. The electrical conductivity of the electrolyte, σ, is assumed to be constant.

The mathematical problem for plating of a cylinder is then reduced to the computation of forced convective transport of reactant to the surface of the cylinder. The system of equations to be solved for the velocity field $\mathbf{u}(\mathbf{u} = u\mathbf{e}_x + v\mathbf{e}_y)$, the pressure field p, the concentration c of the electroactive species and the electric current are
(1) the Navier–Stokes equations,

$$\frac{\partial \mathbf{u}}{\partial t} + (\mathbf{u}\cdot\nabla)\mathbf{u} = -\frac{1}{\rho}\nabla p + \nu\nabla^2\mathbf{u} + \frac{1}{\rho}\mathbf{j}\times\mathbf{B}, \tag{1}$$

where the Lorentz volume force, $\mathbf{j}\times\mathbf{B}$, is due to the magnetic field $\mathbf{B}$ and the current density $\mathbf{j}$. ρ is the density of the electrolyte and ν its kinematic viscosity. In this work, only action of the magnetic field on the mass transport is considered. The modifications of the physical properties of the electrolyte and the electrode kinetics are neglected. Also, only the applied magnetic field B_0 will be considered. The induced magnetic field and the induced current can be shown to be negligible.
(2) the continuity equation for incompressible flow,

$$\nabla\cdot\mathbf{u} = 0, \tag{2}$$

(3) the mass transport, governed by the convection–diffusion equation,

$$\frac{\partial c}{\partial t} + \mathbf{u}\cdot\nabla c = D\nabla^2 c, \tag{3}$$

where D is the molecular diffusivity.
(4) The equation for charge conservation, considering that the electrolyte is electroneutral, may be written as

$$\nabla\cdot\mathbf{j} = 0. \tag{4}$$

The electric current present in an electrolyte is due to the transport of ionic species. This transport is generally caused by three mechanisms: *convection* ($c\mathbf{u}$), *diffusion* ($-D\nabla c$) and *migration* ($-(n_{ea}FD)/(RT)\nabla\Phi$). Here F is the Faraday constant, R the gas constant and T the absolute temperature, which is assumed to be constant, Φ is the electric potential in the electrolyte and n_{ea} the

charge number of the electroactive species. As convection carries an electroneutral solution, the processes that actually transport electric charge in the bath are, in the homogeneous bulk flow only, migration under the imposed electric field **E**, and in the vicinity of the cathode, both diffusion due to the concentration gradient, and migration [7]. As, by assumptions, there is only one species reacting at the cathode, the current density may be written as the sum of two terms, the first due to the local diffusion and the other due to a global migration. This is expressed as

$$\mathbf{j} = -n_{\mathrm{ea}}FD\nabla c + \sigma\mathbf{E} = -n_{\mathrm{ea}}FD\nabla c - \sigma\nabla\Phi. \tag{5}$$

The mathematical difficulty of the problem comes from the coupling between all Equations (1–4) and the term **j** that is related to c.

From Equation 5, making a substitution of variables, the current density can be rewritten in the following form

$$\mathbf{j} = -\sigma\nabla\left(\frac{n_{\mathrm{ea}}FD}{\sigma}c + \Phi\right) = -\sigma\nabla f, \tag{6}$$

where the scalar function f appears as an 'effective' potential, see [8]. The Lorentz force is therefore written as

$$\mathbf{j}\times\mathbf{B} = -\sigma\nabla f\times\mathbf{B}. \tag{7}$$

Equations 1 and 4 may now be rewritten on the form

$$\frac{\partial\mathbf{u}}{\partial t} + (\mathbf{u}\cdot\nabla)\mathbf{u} = -\frac{1}{\rho}\nabla p + \nu\nabla^2\mathbf{u} - \frac{\sigma}{\rho}\nabla f\times\mathbf{B}, \tag{8}$$

$$\nabla^2 f = 0. \tag{9}$$

The boundary condition on the cylinder wall is, for the velocity

$$\mathbf{u} = \mathbf{0}. \tag{10}$$

For the concentration boundary condition at the cylinder, the reaction rate is modeled by an expression of the following, commonly used, form

$$D\mathbf{n}\cdot\nabla c = kc_{\mathrm{w}}. \tag{11}$$

In this expression, **n** is a wall-normal vector, k the *reaction rate* coefficient and c_{w} the value of the concentration at the wall of the cylinder. In the present work we consider cases of high current densities, such that the limiting current density is approached. The concentration of the reduced ions at the surface of the cylinder is thus taken to be zero, i.e.

$$c = 0. \tag{12}$$

In addition, a boundary condition for the 'effective' potential f must be specified. In mass transport limited regime, the current density close to the electrode interface is fully attributed to the diffusion process. The boundary condition for f is thus

$$\mathbf{n}\cdot\mathbf{j} = \mathbf{n}\cdot nFD\nabla c = \mathbf{n}\cdot\sigma\nabla f. \tag{13}$$

As c is constant at the cathode surface, $c = 0$, ∇c has only a normal component. This is true only at the cylinder surface. ∇f (and thus **j**) will be explicitly computed in the whole domain. The computational domain is taken large enough so that current densities in the region close to the inlet are so weak that they cannot influence the imposed inlet hydrodynamics.

In what follows, the cylinder is assumed to be long compared to its diameter so that the problem can be modeled as two-dimensional.

The diffusion coefficient of the electroactive species, D, is constant and has a low value ($D = 5\times 10^{-10}$ m^2 s^{-1}) compared to the fluid kinematic viscosity ($\nu = 10^{-6}$ m^2 s^{-1}). This leads to high value of the Schmidt number, Sc,

$$Sc = \frac{\nu}{D} = 2\times 10^3. \tag{14}$$

Since the Schmidt number is high, the mass transfer boundary layer will be thinner than the corresponding hydrodynamic layer. For typical electrolytes, the ratio between the thickness of the diffusion boundary layer and that of the hydrodynamic boundary layer, respectively, is of the order of 10^{-1} [9].

The following set of suitable variables is used to transform the above equations into a dimensionless form

- the diameter of the cylinder, L_0
- the far-field velocity, U_0
- the far-field concentration of the electroactive species, C_0
- the dynamic pressure, ρU_0^2
- the imposed external magnetic field, B_0
- a reference potential, $f_0 = nFDC_0/\sigma$
- the convective time scale, L_0/U_0.

A time-scale for the diffusion layer can be estimated by

$$t_{\mathrm{D}} \sim \frac{\delta_{\mathrm{D}}^2}{D}. \tag{15}$$

Here δ_{D}, the thickness of the mass transfer boundary layer, may be obtained by balancing the convective mass flux in the tangential direction and the diffusive mass flux in the normal direction [2] whereby one finds that:

$$\delta_{\mathrm{D}} \sim \delta_{\mathrm{H}}Sc^{-1/3} \quad \text{and} \quad \delta_{\mathrm{H}} \sim L_0Re^{-1/2}, \tag{16}$$

where δ_{H} is the thickness of the hydrodynamic boundary layer and Re is the Reynolds number.

Equation 15 can then be written as:

$$t_{\mathrm{D}} \sim \frac{\delta_{\mathrm{D}}^2}{D} \sim \frac{L_0^2Re^{-1}Sc^{-2/3}}{D}. \tag{17}$$

The dimensionless versions of the governing equations are

$$\nabla \cdot \mathbf{u} = 0, \tag{18}$$

$$\frac{\partial \mathbf{u}}{\partial t} + (\mathbf{u} \cdot \nabla)\mathbf{u} = -\nabla p + \frac{1}{Re}\nabla^2 \mathbf{u} - \frac{M_D}{Re^2 Sc}\nabla f \times \mathbf{B}, \tag{19}$$

$$\frac{\partial c}{\partial t} + \mathbf{u} \cdot \nabla c = \frac{1}{Pe}\nabla^2 c, \tag{20}$$

$$\nabla^2 f = 0. \tag{21}$$

The Reynolds and Peclet numbers, Re and Pe, respectively, are defined as

$$Re = \frac{\rho U_0 L}{\mu} \quad \text{and} \quad Pe = \frac{U_0 L}{D}. \tag{22}$$

The dimensionless number M_D, called the magneto-diffusion parameter, is defined as

$$M_D = \frac{nFC_0 B_0 L^2}{\mu}, \tag{23}$$

where μ is the dynamic viscosity of the electrolyte.

The dimensionless time-scale for diffusion $\tau_D = t_D U_0/L_0$ is thus independent of the Reynolds number and takes the very simple form

$$\tau_D = Sc^{1/3} \tag{24}$$

The dimensionless boundary conditions are

$$\mathbf{u} = \mathbf{0}, \quad c = 0 \tag{25}$$

$$\mathbf{n} \cdot \nabla f = \mathbf{n} \cdot \nabla c \tag{26}$$

In the following, only dimensionless variables will be used unless explicitly indicated otherwise.

3. Numerical procedure

The set of equations was solved numerically using the commercially available numerical code, CFX 4.3 [10]. The solution methodology is based on the finite-volume discretization of the transport equations and the continuity equation for an incompressible fluid, resulting in a discrete set of equations for velocity, pressure and concentration.

As magnetoelectrolysis, like MHD, is not available as a simple option of the code features, electro-magnetic effects had to be properly described within the code. A few external mesh points have been implemented for evaluations of gradients in the domain close to the boundaries and right at the boundaries. For example in the source term $(M_D/Re^2 Sc)\nabla f \times \mathbf{B}$ in the Navier–Stokes equations, which is the non-dimensional Lorentz forces, the gradient of f must be evaluated numerically across the domain.

Although CFX is made for dimensional treatment of engineering problems, it was applied to the dimensionless formulation of the problem.

CFX uses multi-block structured grid system for modeling of complex geometries. All variables are defined at the center of control volumes. The domain structure, shown in Figure 1, was produced using *Meshbuild*. A very fine mesh is used close to the cylinder in order to get at least a few cells in the thin concentration boundary layer. To examine effects of the spatial resolution on the results, simulations were carried out using different computational meshes with number of elements varying from 7250 to 24 780. Finally, a grid with 18 450 elements was chosen as finer meshes did not produce any noticeable change in the solution. Four different versions of grids have been used, with different block configurations depending on magnetic field application zones, all having the same cells configuration in the region close to the cylinder.

The numerical scheme is based on the pressure correction method where a correction to the pressure field is computed such that the divergence of the velocity field is forced to be zero and the continuity equation can be satisfied. At each time step the nonlinear equations are solved by iteration. The convection velocity and other parameters are evaluated at the previous iteration and a linear equation system is formed for each variable. The linearized difference equation system is solved by an iterative solution method.

Third-order differencing schemes were used for the convection terms.

Figure 2 shows the computational domain with the block structures and boundary conditions.

4. Results and discussion

The numerical computations were carried out for $Re = 10$, at limiting current conditions, i.e. the interfacial concentration of the reduced ions is constant and equal to zero along the cathode surface.

The physical parameters are chosen to be as close as possible to industrial applications of electrodeposition of gold on electrical connectors. The cylinder diameter is 1 mm. The physical properties of the electrolyte are: density $\rho = 10^3$ kg m^{-3}, kinematic viscosity $\nu = 10^{-6}$ m^2 s^{-1} and diffusion coefficient of the gold ions in the electrolyte $D = 5 \times 10^{-10}$ m^2 s^{-1}. The Schmidt number is 2000.

To compare cases where a magnetic field is applied with the case without magnetic field, the distributions of mass transfer are compared to a reference case defined as follows: the distribution of deposit thickness on the cylinder obtained during the time interval T_1 required to set up a layer of thickness 1 μm at the forward

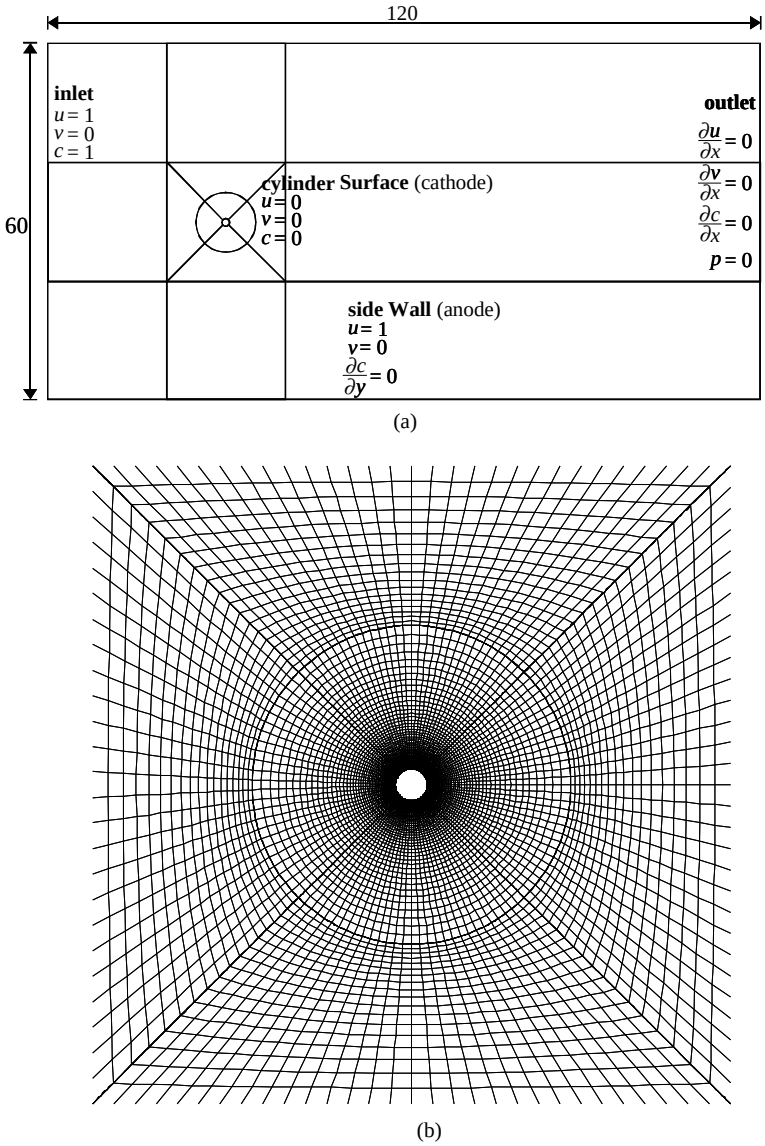

Fig. 2. (a) Computational domain, mesh structure, and boundary conditions. (b) Mesh on the eight blocks around the cylinder.

stagnation point of the cylinder. T_1 is computed from the simulation of the case with $\mathbf{B} = 0$ at $Re = 10$. Also, as the initial guess for computed simulations cannot reflect the complex phenomena happening when the cathodes plunge in the electrolytic bath. The problems due to initial transients were avoided by considering a time interval starting at $t_1 = \tau_D$, corresponding to the time-scale for the diffusion layer. From the parameter values given above, one finds that

$$\tau_D = Sc^{1/3} = 12.6. \tag{27}$$

The objective of this work is to examine the possibility of enforcing various kinds of swirling motions of the electrolyte around the cylinder in order to obtain a more homogeneous mass transfer. It will be shown later that this concept can indeed be made successful.

For this purpose, a longitudinal, i.e. parallel with the axis of the cylinder, magnetic field that induces a Lorentz force that is directed around the cylinder is chosen, see Figure 3. As this force field is perpendicular to the radial electric current field, it tends to set up a circulatory motion in planes that are perpendicular to the axis of the cylinder. The force is proportional to the intensity of the electric current density, cf. Equation 1, and is therefore most efficient in the vicinity of the cylinder.

4.1. *A homogeneous steady magnetic field*

In this case, a constant and time-independent external magnetic field is imposed in the whole electrolytic bath. Different values of magnetic field intensity were investigated, corresponding to values of M_D/Re^2Sc between 10^{-3} and 5×10^{-2}. The computed distributions of deposit thickness at the cylinder surface are shown in Figure 4. It can be seen that when M_D/Re^2Sc is of the order of 10^{-3}, the effect of the Lorentz force on the flow is just a very small rotation of the mass transfer distribution. The thickness distribution has two minimum

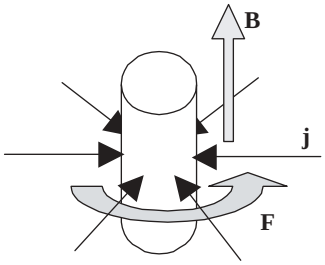

Fig. 3. Application of a longitudinal magnetic field that induces Lorentz forces that tend to spin the electrolyte around the cylinder.

values located at the separation points in the rear part of the cylinder (near 25° and 335°), see [1]. Instead of the two small eddies that are formed when no force is applied, only one is formed, see Figures 5a and 5b. For higher values of the magneto-diffusion parameter, the structure of the flow and concentration fields is significantly changed. The flow becomes notably asymmetric, the downstream eddies are removed and the flow tends to be wrapped around the cylinder. There is only one separation point in the rear part of the cylinder, see Figure 5b. When M_D/Re^2Sc is increased to 5×10^{-2}, the flow above the cylinder is practically reversed but does not reach a state where the cylinder is enclosed by streamlines. This is due to the extent of the zone where the Lorentz force acts, which is here the whole bath. The Lorentz force drives a large scale complex flow where, on one side of the cylinder the flow is taken from 'downstream' to 'upstream' while on the other side the force speeds up the flow, making it impossible for the electrolyte to move in closed streamlines around the cylinder. The homogenization of the deposit layer shown in Figure 4 can hardly be characterized as successful.

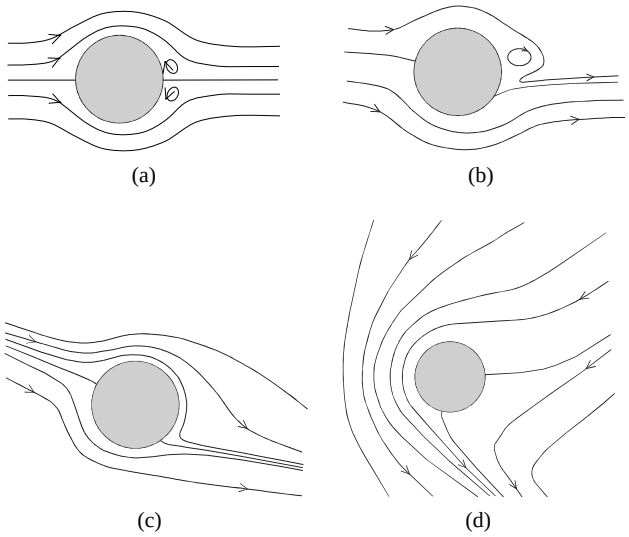

Fig. 5. Flow structure for different values of the magnetic field intensity. The values of M_D/Re^2Sc are 0 (a), 10^{-3} (b), 10^{-2} (c), 5×10^{-2} (d).

No value larger than 5×10^{-2} of M_D/Re^2Sc could be simulated. For larger values of this parameter, the Lorentz force distorts the motion of the electrolyte into such complexity that the assumption of steady motion appears to break down. This seems to be a reasonable explanation for the lack of convergence of the computer code.

There are thus good reasons to modify the structure of the magnetic field.

4.2. *A localized steady magnetic field*

The simulations presented in the previous section show that it is not possible to obtain closed streamlines around

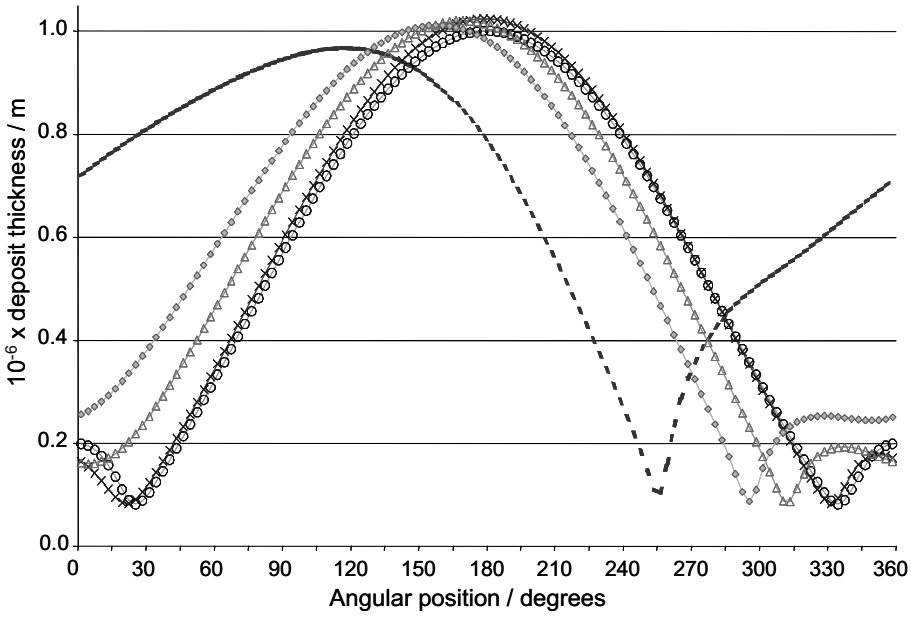

Fig. 4. Distribution of the deposit thickness on the cylinder for various intensities of the magnetic field at Re=10. The values of M_D/Re^2Sc are: 0.0 (–○–), 0.001 (–×–), 0.01 (–△–), 0.02 (–◇–), 0.05 (- - - -). The zero angle corresponds to the front stagnation point.

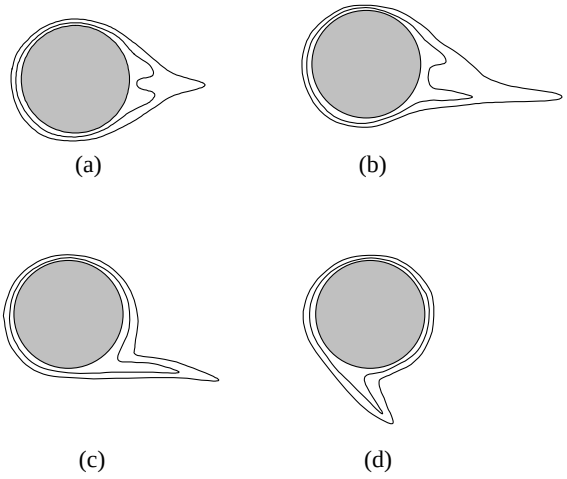

Fig. 6. Structure of the concentration field for different values of the magnetic field intensity. The values of M_D/Re^2Sc are the same as in Figure 5.

the cylinder with an electro-magnetic Lorentz force acting on the whole bath of electrolyte. However, there are reasons to believe that this type of flow can be obtained by constraining the spatial distribution of the Lorentz force to a limited zone around the cylinder. For this purpose, the region where the axial magnetic field is non-zero was limited to a circular zone around the cylinder, see Figure 7. The radial distance between the surface of the cylinder and the boundary of the magnetic field is e.

The flow type and the resulting distribution of mass flux to the cylinder now depend on both M_D/Re^2Sc and

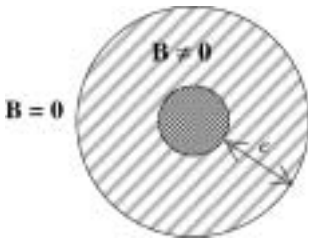

Fig. 7. Zone where the magnetic field is applied.

e. The computed results are summarized in Table 1 and Figure 8.

- When the level of the magnetic field is low ($M_D/Re^2Sc = 10^{-2}$), the Lorentz force just slightly displaces the separation points. For $e = L_0$ (Table 1, case (a)), a small eddy is formed downstream of the cylinder, quite similar to the case where the magnetic field is applied in the whole bath, see Figure 5a. However, the eddy is moved from $y > 0$ to $y < 0$. When e is smaller, i.e. $e = L_0/2$ and $e = L_0/4$, see Table 1 cases (b) and (c), there are two separation points, both of these are located in $y > 0$.
- For higher values of M_D/Re^2Sc, a closed recirculation zone around the cylinder can be obtained for certain values of e. If e is large, $e = L_0$, see Table 1 case (d), the recirculation zone is also large and an eddy appears there for $M_D/Re^2Sc = 10^{-1}$. The eddy disappears for $e = L_0/2$, see Table 1 case (e). On the other hand, if the zone of application of the magnetic field is too small, $e = L_0/4$, the net

Table 1. Types of flow obtained with different values of M_D/Re^2Sc and the gap e, $Re = 10$

M_D $/Re^2\ Sc$	$e = L_0$	$e = L_0/2$	$e = L_0/4$
10^{-2}	(a)	(b)	(c)
10^{-1}	(d)	(e)	(f)
1			(g)

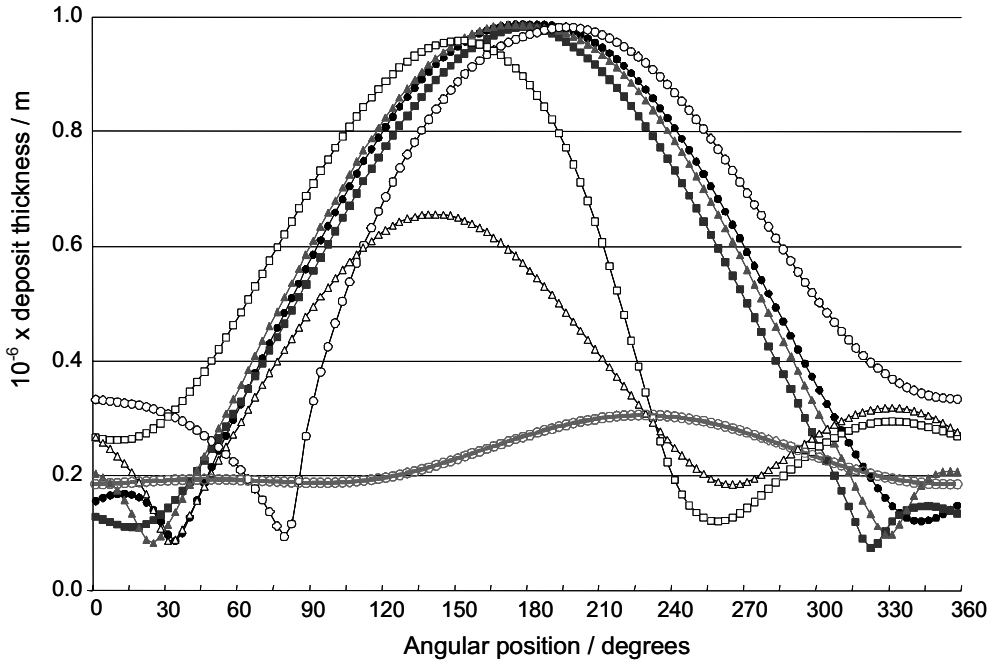

Fig. 8. Distribution of the deposit thickness on the cylinder for various intensities of the localized magnetic field and of the distance of the magnetic field boundary e, $Re = 10$. The values of M_D/Re^2Sc (and e) are: 0.01 ($e = R/2$) (–●–), 0.01 ($e = R$) (–■–), 0.01 ($e = 2R$) (–▲–), 0.1 ($e = R/2$) (–○–), 0.1 ($e = R$) (–◇–), 0.1 ($e = 2R$) (–△–), 1.0 ($e = R/2$) (- -○- -).

Lorentz force is also too small and the streamlines cannot completely enclose the cylinder, see Table 1 case (f).

– A case with a very high value of the magneto-diffusion parameter, $M_D/Re^2Sc = 1$, was computed, see case (g) in Table 1 and the corresponding distribution of deposit in Figure 8. In this case, the motion of the electrolyte is strong and the resulting mass flux distribution is almost homogeneous, unfortunately at a low level. The reason for this low level is that the closed recirculating zone around the cylinder is relatively large and that the diffusion boundary layer can extend to such a distance. The difference with the case (e) is that in the case (e) the speed of the rotating fluid is lower than in case (g), the size of the circulating zone is smaller but the ratio between the maximum and minimum thickness of the boundary layer is important. For case (g), the boundary layer, and diffusion layer, is thicker but the ratio between maxi and minimum thickness is inferior; the net result is thus that the mass transfer is lower, but more homogeneous, see Figure 8.

The use of a magnetic field applied locally around the cylinder shows that it is possible to obtain a forced circulation around the cylinder surface. However, some limitations of this concept are

– the resulting distribution of mass transfer is either notably non-homogeneous or relatively low, see Figure 8,
– the intensity of the magnetic field necessary to obtain a closed circulation is relatively high, around 1 T or more,
– it would be technically difficult to set up a magnetic field that is concentrated in a limited zone around the small cylinder.

4.3. *Alternating magnetic field*

In the previous subsections it was shown that it is possible to obtain a closed zone of circulating electrolyte around the cylinder. However, this state is difficult to obtain due to the need for a localized and relatively strong magnetic field. Also the deposit distribution is not satisfying, either in terms of homogeneity or in terms of overall rate of mass transfer.

On the other hand, for a steady homogeneous magnetic field, it was shown in Section 4.1., see Figure 4, that, when the magneto-diffusion parameter is high enough ($M_D/Re^2Sc = 0.05$), the distribution of the wall mass transfer reaches a state that one may characterize as 'nearly anti-symmetrical' with most of the deposit located on the upper part of the cylinder. This interesting fact suggests consideration of a homogeneous but alternating magnetic field. The purpose would be to switch between two states of flow. One of these would be similar to that shown in Figure 5c and the other one its mirror image in the y-axis. This would effectively act like an oscillatory rotation of the cylinder in the case $\mathbf{B} = 0$ but now with a rotation of the stagnation points by something like $\pm 90°$. With reference to the flow field shown in Figure 5c, it turns out to be possible to set up oscillations like those sketched in Figure 9. An unexpected advantage, compared to rotating cylinder with $\mathbf{B} = 0$, is that, due to the Lorentz force around the

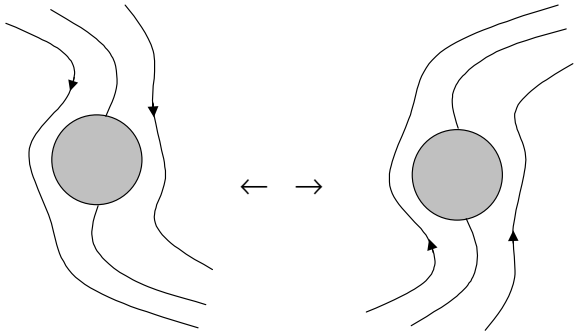

Fig. 9. Schematic representation of two peak states in a switched flow.

cylinder, no eddies appear. As was pointed out in Section 4.1, eddies are detrimental to the homogeneity of the deposit.

4.3.1. *Estimates of switching time T and magnitude of B*
Obviously, the non-dimensional time delay T between each switch of the direction of **B** should be longer than the non-dimensional diffusion time scale τ_D, so that there is enough time to set up a diffusion layer, i.e.

$$\tau_D \leqslant T. \tag{28}$$

According to (27), τ_D is of the order of 10. It is then obvious that the changes in the flow conditions should have a half-period of at least 10, i.e. $T \geqslant 20$. On the other hand, to get an 'averaging' effect, the total time of the plating process as a whole, which is about 500, should enclose a number of periods. Thus, the period of the alternating applied magnetic field, T, should be in a range

$$20 \leqslant T \leqslant 200. \tag{29}$$

There is another time-scale that depends on the intensity of the magnetic field. Each time the direction of the applied magnetic field is reversed, the flow field must have enough time to adjust to this change. An estimate of the dimensional time-scale t^* needed for the flow adjustment to the periodic reversals of **B**, may be obtained by considering a balance between the Lorentz force, of the order of (jB), and the inertia of the fluid flow, of the order of $(\rho\, L/t^{*2})$, i.e.

$$jB \sim \rho L/t^{*2}. \tag{30}$$

An estimate of j may be obtained by a linear approximation of the concentration gradient in the diffusive boundary layer

$$j \sim \frac{zFDC_0}{\delta_D}, \tag{31}$$

with δ_D given by Equation 16. This gives the following *non-dimensional* estimate of t^* (the time scale being L_0/U_0)

$$t^* \sim \sqrt{\frac{Re^{3/2}Sc^{2/3}}{M_D}}. \tag{32}$$

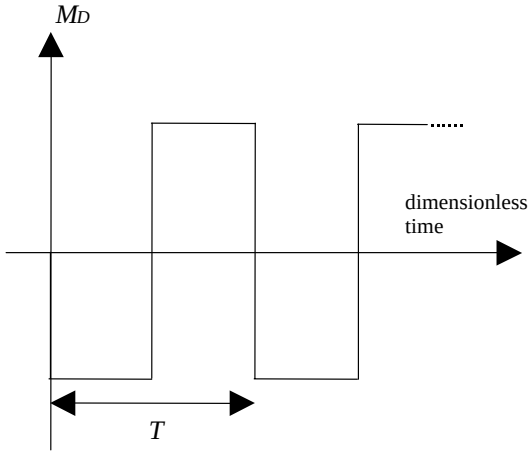

Fig. 10. The alternating applied magnetic field.

The half period of the applied magnetic field, $T/2$, should be larger than t^*, which gives that

$$\frac{Re^{3/2}Sc^{2/3}}{M_D} < \frac{T^2}{4}. \tag{33}$$

For a given value T in the range specified in Equation 29, this gives an estimate of the minimum value for M_D. For $T = 20$, one obtains, with $Re = 10$ and $Sc = 2 \times 10^3$,

$$M_D > 10^2 \quad \text{or} \quad \frac{M_D}{Re^2 Sc} > 10^{-3}. \tag{34}$$

In this work, a 'square' wave signal, see Figure 10, was chosen for the magnetic field as this maximizes the effectiveness of changes in direction.

In reality, it is not possible to generate an idealized square wave of a magnetic field with abrupt changes of direction. By considering that the field inversion is not abrupt but takes a short time, for example $T/10$, the induced electric field generated during the inversion time can be shown to be very small compared with the applied electric field. This is a consequence of the extremely low frequency, lower than 1 Hz, which is required for good working of the suggested process. Accordingly, the induced electric field is neglected in the following.

4.3.2. *Result*
Figure 11 shows the distribution of the deposit thickness for various values of the magneto-diffusion parameter for a fixed period $T = 200$. As expected, a weak oscillating Lorentz force just smoothes out the distinct minima in the rear part of the cylinder. When the Lorentz force is stronger, $M_D/Re^2Sc = 5 \times 10^{-2}$, the switching between the states sketched in Figure 9 tends to distribute the strongly asymmetric distribution shown in Figure 4 on *both* the upper and lower parts of the cylinder. As can be seen from Figure 11, this results in a

distribution that is much more homogeneous compared to the standard case.

Figure 12 shows the effect of the period T. It can be seen that if the period is too short (or the frequency too high), e.g. $T = 20$, the slow adjustment of the diffusion layer cannot keep up with the flow oscillations generated by the alternating magnetic field. To the contrary, for longer values of the period T, the averaging effect of the oscillations is clearly demonstrated.

If the period is very long, this means close to the total time of deposition which is 451 non-dimensional time-units, plating during the non-completed period produces a 'non-symmetrization' of the resulting deposit, see the curve for $T = 400$ in Figure 12.

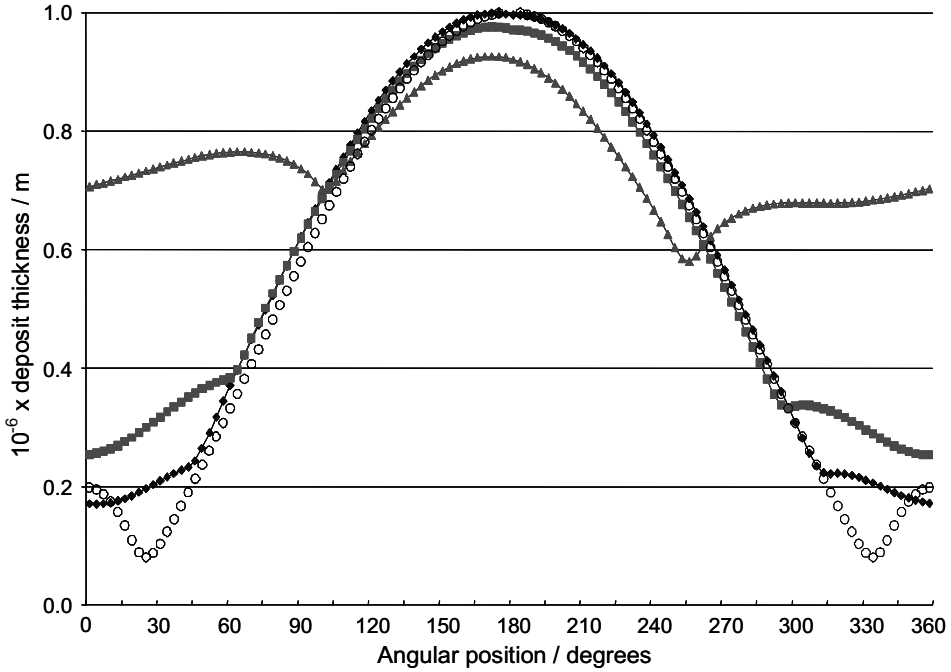

Fig. 11. Distribution of the deposit thickness on the cylinder for various intensities of an alternating magnetic field at $Re = 10$; $T = 200$. The values of M_D/Re^2Sc are: 0.0 (○), 0.01 (–♦–), 0.02 (–■–), 0.05 (–▲–).

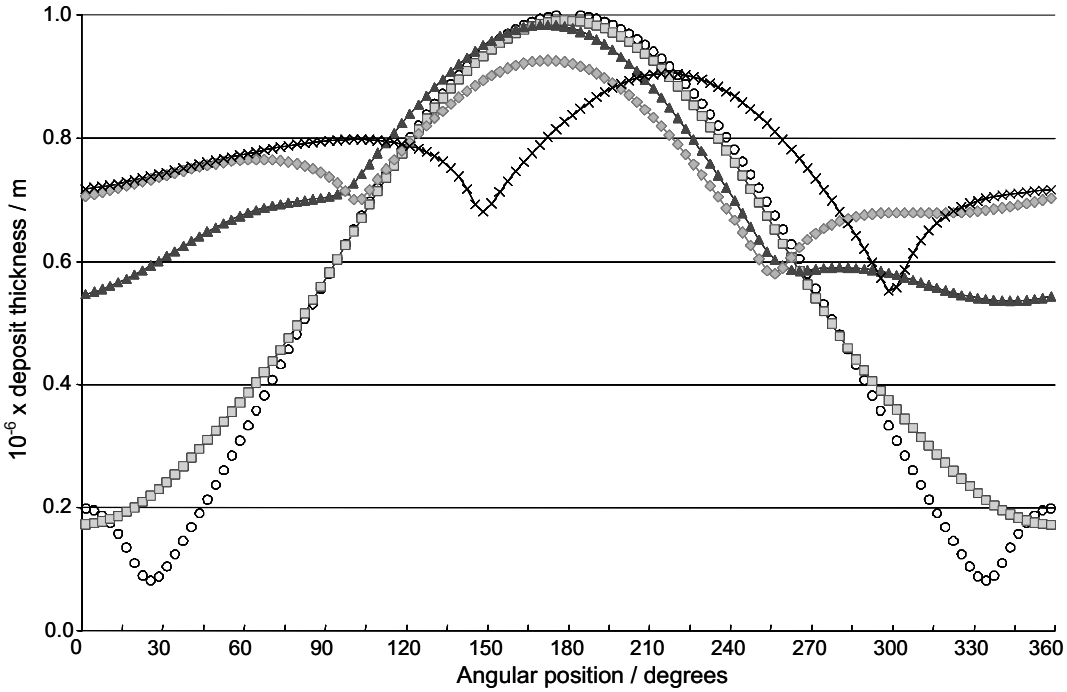

Fig. 12. Distribution of the deposit thickness on the cylinder with alternating magnetic field for various frequencies at $Re = 10$. $M_D/Re^2Sc = 0.05$, $Re = 10$. Total deposition time is 451. The values of the period T are: $T = 20$ (–■–), $T = 100$ (–▲–), $T = 200$ (–♦–), $T = 400$ (–×–), no magnetic field (○).

Fig. 13. Enlarged deposit layer thickness. Limiting current, $Re = 10$. Alternating magnetic field with $T = 200$ and $M_D/Re^2Sc = 0.05$.

Figure 13 shows the distribution of the deposit for the most efficient case ($T = 200$ and $M_D/Re^2Sc = 0.05$) examined in this work. The improvement compared with the case shown in Figure 1 is obvious.

From a quantitative point of view, one may also note that

- The minimum value of the deposit thickness for the case shown in Figure 13 is more than seven times larger than for the reference case.
- Not only is there an improved uniformity of the distribution of the deposit, but the total amount of deposited metal is increased by 36% for the same deposition time.

4.3.3. *Some dimensional parameter values*

The development in this work has, for convenience, been made in terms of non-dimensional variables and parameters. However, certain dimensional values are of interest to assess industrial feasibility of the proposed concept. Examples of such values are given in Table 2 and Table 3.

5. Conclusion

Numerical simulations of electrochemical plating of a single cylinder with forced convection for Reynolds number 10 were performed with a longitudinal, i.e. parallel with the axis of the cylinder, magnetic field applied on the bath. The purpose of this work was to examine the feasibility of such a process for improving the disturbing non-homogeneity of the deposit that normally appears in industrial plating. This non-homogeneity is due to boundary layer and wake effects. Three cases were considered where the magnetic field is applied (i) in the whole bath, (ii) in a local zone around the cylinder and (iii) in the whole bath but with an alternating direction.

When a steady homogeneous magnetic field is applied in the whole domain, it was found that it is not possible to reach a state where circulating motion of the electrolyte around the cylinder is formed. The magnetic force generates a velocity distribution of the fluid flow that extends in a large zone around the cylinder but that corresponds to a rotation of maximum 90° of the flow pattern. No satisfactory improvement of the deposit homogeneity was found.

When a steady magnetic field is applied *locally* around the cylinder, it is possible to find appropriate values for the intensity of the magnetic field and the size of the zone of application so that a closed recirculation around the cylinder is formed. However, it was found that only for a very strong magnetic field can a satisfactory homogeneity of the deposit be obtained. Unfortunately, in such cases, the rate of the mass transfer is severely reduced because the recirculating zone is poorly supplied with electroactive species.

Promising results were obtained by applying the magnetic field in the whole bath but alternating its direction. This case gives not only a good homogenization of the deposit but also a significant improvement of the overall mass transfer rate due to efficient supply of electroactive species from the bath. With optimized values of the magneto-diffusion parameter and of the switching frequency, a notable improvement of the quality of the deposit is obtained, both in terms of homogeneity and productivity.

It can be concluded that, by using a magnetic field, it is possible to considerably improve this kind of industrial electroplating processes. One should also be aware of the fact that, as observed in many experiments, the use of magnetic field improves the metallurgical structure of the deposits.

Table 2. Dimensional values, for $Re = 10$, $n_{ea} = 2$, $C_0 = 0.1$ mol l^{-1}

Cylinder diameter L_0 /mm	1	5	10
Far field velocity U_0/m s^{-1}	10^{-2}	2×10^{-3}	10^{-3}
Magnetic field B/T for $M_D/Re^2Sc = 0.01$	10^{-1}	4×10^{-3}	10^{-3}
Magnetic field B/T for $M_D/Re^2Sc = 0.05$	5×10^{-1}	2×10^{-2}	5×10^{-3}

Table 3. Some dimensional values for frequencies, $Re = 10$

Dimensionless period T	200	200	100	100
Cylinder diameter L_0/mm	1	2	1	2
Dimensional period/s *corresponding to* $T = 200$	20	80	10	40
Dimensional frequency f/Hz	0.05	0.0125	0.1	0.025

References

1. P. Olivas, S. Zahrai and F.H. Bark, *J. Appl. Electrochem.* **27** (1997) 1369.
2. J. Josserand, Thèse Docteur de 1'I.N.P. Grenoble (1994) 84.
3. S. Mori, K. Satoh and A. Tanimoto, *Electrochim. Acta* **39** (1994) 2789.
4. S. Mori, M. Kumita, M. Takeuchi and A. Tanimoto, *J. Chem. Eng. Jpn.* **29** (1996) 229.
5. Z.H. Gu and T.Z. Fahidy, *J. Electrochem. Soc.* **134**(9) (1987) 2241.
6. P. Olivas, Mémoire de D.E.A. de 1'I.N.P. Grenoble (1994).
7. F. Alavyoon, A. Eklund, F.H. Bark, R.I. Karlsson and D. Simonsson, *Electrochim. Acta* **36**(14) (1991) 2153.
8. C.F. Wallgren, F.H. Bark and B.-J. Andersson, *Electrochim Acta* **41**(8) (1996) 2909.
9. V.G. Levich, 'Physicochemical Hydrodynamics' (Prentice Hall, Englewood Cliffs, NJ, 1962) Chapters 2, 6.
10. CFX International, 'CFX 4.2 User Guide' (CFX International, Harwell Laboratories, Oxfordshire, OX11 0RA, UK, 1996).
11. J.P. Celis, M. De Bonte and J.R. Roos, *Trans. I.M.F.* **72**(2) (1994) 89.